MATEC Web of Conferences **189**, 11006 (2018) https://doi.org/10.1051/matecconf/201818911006
MEAMT 2018

Electron transport coefficients in binary mixtures of tetramethylsilane gas with Kr, Xe, He and Ne gases

Phan *Thi Tuoi*, Pham *Xuan Hien*, and Do *Anh Tuan*[*]

Faculty of Electronics and Electrical Engineering, Hung Yen University of Technology and Education, Vietnam

Abstract. Tetramethylsilane, alone and in combination with inert gases are widely used in various material processing. The electron transport coefficients in binary mixtures tetramethylsilane gas with buffer gases such as Kr, Xe, He, and Ne gases, therefore, was firstly calculated and analyzed by a two-term approximation of the Boltzmann equation in the E/N (ratio of the electric field E to the neutral number density) range of 0.1-1000 Td (Townsend). These results can be considered to use in many industrial applications depending on particular application of gas, especially on plasma polymerization and plasma enhanced chemical vapour deposition.

1 Introduction

Tetramethylsilane [(TMS), $Si(CH_3)_4$] vapour is widely used in plasma polymerization and plasma enhanced chemical vapour deposition (PECVD) [1-7]. As analyzed by Kawaguchi *et al* [8], in order to obtain the high hardness and low friction coefficient of thin film, TMS vapour is often used to deposit a thin film of silicon-doped diamond like carbon (Si-DLC) in PECVD processes [9, 10]. These film properties are strongly influenced by the characteristics of the discharge plasma used for film deposition. Therefore, the effects of the plasma characteristics on the film properties have been paid attention by many researchers [11, 12]. Grotjahn *et al* [11] reported that the hardness of the Si-DLC film increases with radio frequency power and flow rate of TMS vapour based on results of film deposition using a capacitively coupled plasma (CCP) in TMS-Ar mixtures. Soum-Graude *et al* [12] also reported that $Si(CH_3)_3$ and C_2H_5 significantly contributes to the growth of the Si-DLC film based on computer the simulation of Si-DLC film deposition by TMS-Ar plasma. This simulation was carried out using the transport and gas-phase reaction of charged and neutral species as well as the surface reaction of neutral species [12]. Steven and Mário [13] investigated the conventional and dynamic actinometry of glow discharges in mixtures of TMS and He, and reported the advantage of using an inert gas in film deposition. Because of above reasons, the electron transport coefficients, which include electron drift velocity, density-normalized longitudinal diffusion coefficient, ratio of longitudinal diffusion coefficient to electron mobility, Townsend first ionization coefficient

[*] Corresponding author: tuandoanh@utehy.edu.vn

in mixtures of TMS and inert gases, were calculated and analyzed using a Boltzmann equation analysis.

2 Analysis

The electron transport coefficients in mixtures of TMS gas and inert gases such as Kr, Xe, He and Ne were calculated using a two-term Boltzmann approximation and data of electron collision cross sections of used mixtures of gases. Since the validity of electron collision cross section set for gaseous molecule is the most fundamental factor in obtaining the reliable electron transport coefficients, the collecting the accurate electron collision cross section set is necessary. Therefore, in this study, we used the electron collision cross section set for TMS molecule, He, Xe, Ne and Kr atoms as listed below. The set for TMS molecule [14] includes one momentum transfer cross section, two vibrational excitation cross sections (threshold energies of 0.15 eV and 0.21 eV), one electronic excitation cross section (threshold energy of 6.5 eV), one dissociative attachment cross section (threshold energy of 3.05 eV) and one ionization cross section (threshold energy of 9.8 eV). The set of electron collision cross sections for Kr atom determined by Hayashi [15] includes one momentum transfer cross section, fourteen electronic excitation cross sections (threshold energies of 9.915 to 13.437 eV) and one total ionization cross section (threshold energy of 14.0 eV). The set of electron collision cross sections for Xe atom determined by Hashimoto and Nakamura [16], includes one momentum transfer, fourteen electronic excitation cross sections (threshold energies of 8.315 to 11.58 eV), and one total ionization cross section (threshold energy of 12.13 eV). In this study, we used the two-term approximation of the Boltzmann equation for the energy given by Tagashira *et al* [17]. This calculated method was successfully used in previous works [14, 18, 19]. Therefore, the calculated electron transport coefficients, which include electron drift velocity, density-normalized longitudinal diffusion coefficient, ratio of longitudinal diffusion coefficient to electron mobility, and Townsend first ionization coefficient in mixtures of TMS molecule with He, Xe, Ne and Kr atoms, are reliable.

3 Results and discussions

The results for the electron transport coefficients, as functions of E/N for mixtures of TMS with He, Xe, Ne and Kr, calculated in the wide E/N range by a two-term approximation of the Boltzmann equation are shown in figures 1-4. The calculated electron drift velocities in mixtures are suggested to be between those of the pure gases over the range of E/N > 100Td (for TMS-Kr and TMS-Xe mixtures) and over the range of E/N > 20 Td (for TMS-He and TMS-Ne mixtures). In the range of E/N ≤ 20 Td in figures 1 and 2, the values of W in TMS-Kr and TMS-Xe mixtures are higher than those in TMS, Kr and Xe gases. Similarly mentioned by Tuan [18], the electron drift velocity strongly depends on the momentum transfer and vibrational excitation cross sections. In this range of E/N, the vibrational excitation occurred, the momentum transfer cross section of TMS molecule is higher than that of Kr and Xe atoms and the momentum transfer cross sections of Kr and Xe atoms are deeply decreasing to the minimum points. Therefore, the curves of W in mixtures have same tendency as that in pure TMS molecule. As shown in figures 3 and 4 most values of W in TMS-He and TMS-Ne mixture gases are suggested to be between those of the pure gases over the all range of E/N, exception in 10%, 30% or 50% TMS-He and TMS-Ne mixtures. For these cases, the reasons could be suggested that in this range of E/N, the momentum transfer cross section of TMS molecule is higher than that of He and

Ne atoms and the momentum transfer cross sections of He and Ne gases are slightly increasing.

The calculated density-normalized longitudinal diffusion coefficients and ratio of the longitudinal diffusion coefficients to the electron mobility and the first Townsend ionization coefficients in TMS-Kr, TMS-Xe, TMS-He and TMS-Ne mixtures are shown in figures 5-16. These coefficients in the mixtures are suggested to be between those of the pure gases over the all range of E/N.

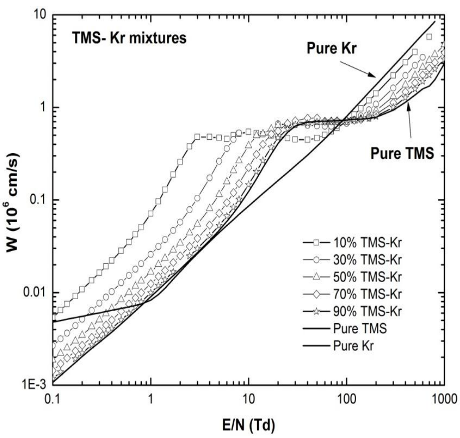

Fig. 1. The electron drift velocity, W, as a function of E/N for the TMS-Kr mixtures with 10%, 30%, 50%, 70%, and 90% TMS. The solid line and symbols show present W values calculated using a two-term approximation of the Boltzmann equation for the TMS-Kr mixtures. The solid curves show present W values calculated for the pure TMS molecule and Kr atom.

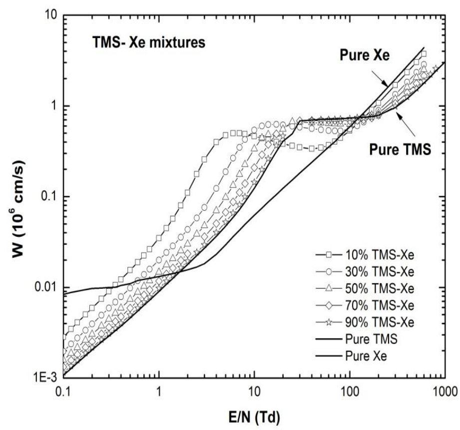

Fig. 2. The electron drift velocity, W, as a function of E/N for the TMS-Xe mixtures with 10%, 30%, 50%, 70%, and 90% TMS. The solid line and symbols show present W values calculated using a two-term approximation of the Boltzmann equation for the TMS-Xe mixtures. The solid curves show present W values calculated for the pure TMS molecule and Xe atom.

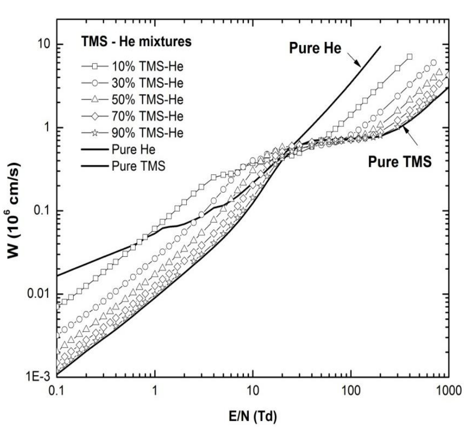

Fig. 3. The electron drift velocity, W, as a function of E/N for the TMS-He mixtures with 10%, 30%, 50%, 70%, and 90% TMS. The solid line and symbols show present W values calculated using a two-term approximation of the Boltzmann equation for the TMS-He mixtures. The solid curves show present W

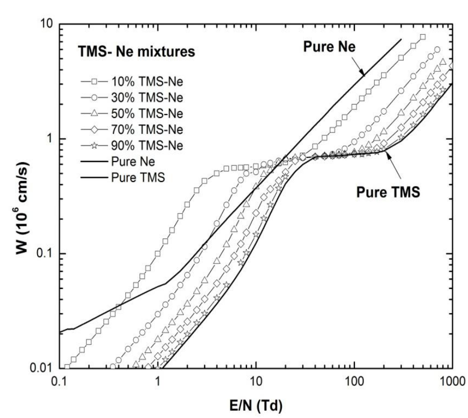

Fig. 4. The electron drift velocity, W, as a function of E/N for the TMS-Ne mixtures with 10%, 30%, 50%, 70%, and 90% TMS. The solid line and symbols show present W values calculated using a two-term approximation of the Boltzmann equation for the TMS-Ne mixtures. The solid curves show

values calculated for the pure TMS molecule and He atom.

present W values calculated for the pure TMS molecule and Ne atom.

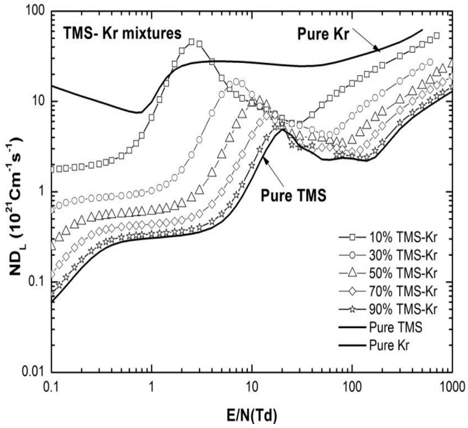

Fig. 5. The density-normalized longitudinal diffusion coefficient, ND_L, as a function of E/N for the TMS-Kr mixtures with 10%, 30%, 50%, 70%, and 90% TMS. The solid line and symbols show present ND_L values calculated using a two-term approximation of the Boltzmann equation for the TMS-Kr mixtures. The solid curves show present ND_L values calculated for the pure TMS molecule and Kr atom.

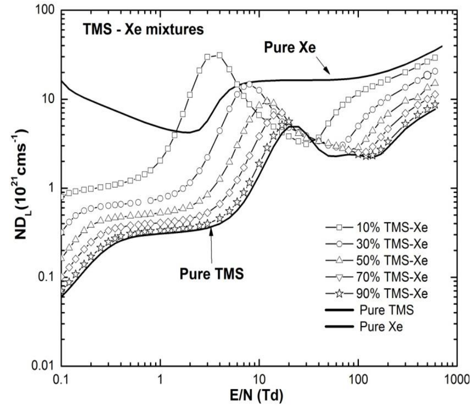

Fig. 6. The density-normalized longitudinal diffusion coefficient, ND_L, as a function of E/N for the TMS-Xe mixtures with 10%, 30%, 50%, 70%, and 90% TMS. The solid line and symbols show present ND_L values calculated using a two-term approximation of the Boltzmann equation for the TMS-Xe mixtures. The solid curves show present ND_L values calculated for the pure TMS molecule and Xe atom.

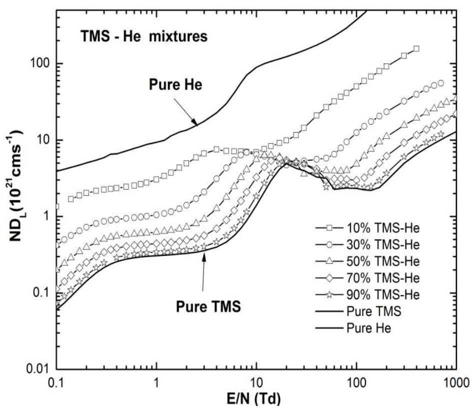

Fig. 7. The density-normalized longitudinal diffusion coefficient, ND_L, as a function of E/N for the TMS-He mixtures with 10%, 30%, 50%, 70%, and 90% TMS. The solid line and symbols show present ND_L values calculated using a two-term approximation of the Boltzmann equation for the TMS-He mixtures. The solid curves show present ND_L values calculated for the pure TMS molecule and He atom.

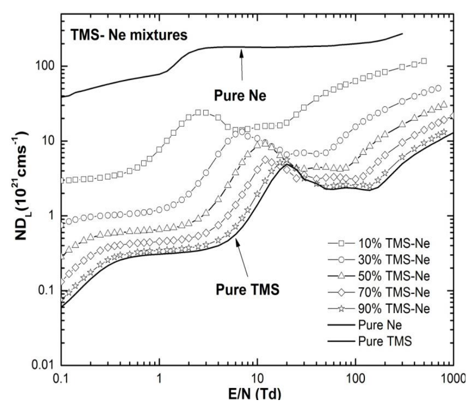

Fig. 8. The density-normalized longitudinal diffusion coefficient, ND_L, as a function of E/N for the TMS-Ne mixtures with 10%, 30%, 50%, 70%, and 90% TMS. The solid line and symbols show present ND_L values calculated using a two-term approximation of the Boltzmann equation for the TMS-Ne mixtures. The solid curves show present ND_L values calculated for the pure TMS molecule and Ne atom.

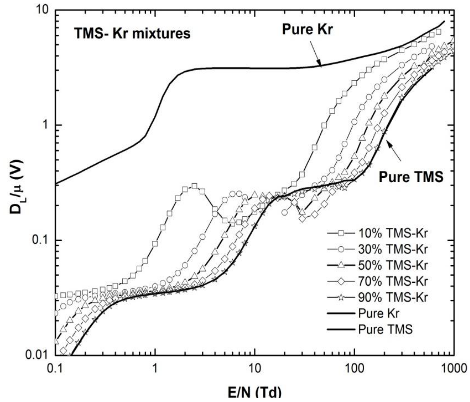

Fig. 9. Ratio of the longitudinal diffusion coefficient to the mobility, D_L/μ, as a function of E/N for the TMS-Kr mixtures with 10%, 30%, 50%, and 70%, and 90% TMS. The solid line and symbols show present D_L/μ values calculated using a two-term approximation of the Boltzmann equation for the TMS-Kr mixtures. The solid curves show present D_L/μ values calculated for the pure TMS and Kr molecules.

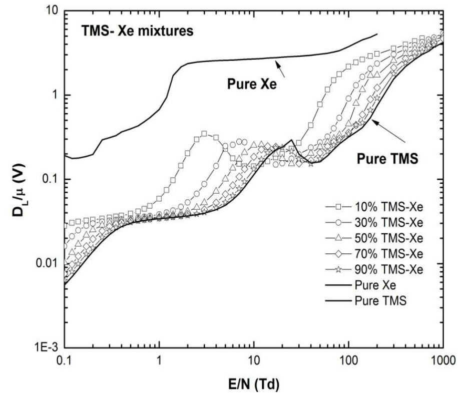

Fig. 10. Ratio of the longitudinal diffusion coefficient to the mobility, D_L/μ, as a function of E/N for the TMS-Xe mixtures with 10%, 30%, 50%, and 70%, and 90% TMS. The solid line and symbols show present D_L/μ values calculated using a two-term approximation of the Boltzmann equation for the TMS-Xe mixtures. The solid curves show present D_L/μ values calculated for the pure TMS and Xe molecules.

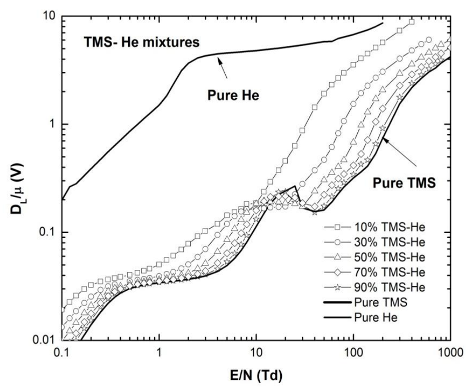

Fig. 11. Ratio of the longitudinal diffusion coefficient to the mobility, D_L/μ, as a function of E/N for the TMS-He mixtures with 10%, 30%, 50%, and 70%, and 90% TMS. The solid line and symbols show present D_L/μ values calculated using a two-term approximation of the Boltzmann equation for the TMS-He mixtures. The solid curves show present D_L/μ values calculated for the pure TMS and He molecules.

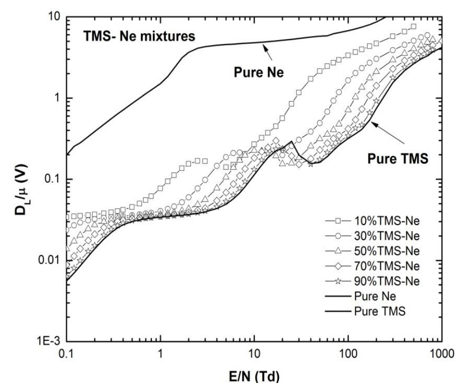

Fig. 12. Ratio of the longitudinal diffusion coefficient to the mobility, D_L/μ, as a function of E/N for the TMS-Ne mixtures with 10%, 30%, 50%, and 70%, and 90% TMS. The solid line and symbols show present D_L/μ values calculated using a two-term approximation of the Boltzmann equation for the TMS-Ne mixtures. The solid curves show present D_L/μ values calculated for the pure TMS and Ne molecules.

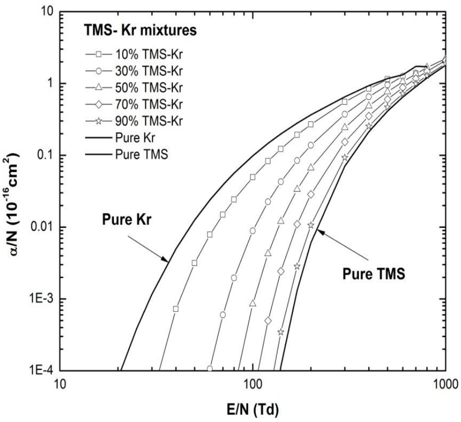

Fig. 13. The first Townsend ionization coefficient, α/N, as a function of E/N for the TMS-Kr mixtures with 10%, 30%, 50%, 70%, and 90% TMS. The solid line and symbols show present α/N values calculated using a two-term approximation of the Boltzmann equation for the TMS-Kr mixtures. The solid curves show the present α/N values calculated for pure TMS and Kr.

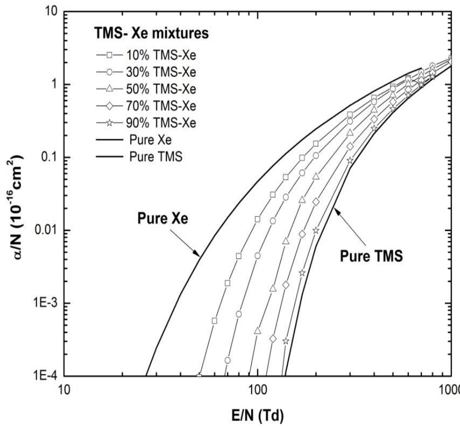

Fig. 14. The first Townsend ionization coefficient, α/N, as a function of E/N for the TMS-Xe mixtures with 10%, 30%, 50%, 70%, and 90% TMS. The solid line and symbols show present α/N values calculated using a two-term approximation of the Boltzmann equation for the TMS-Xe mixtures. The solid curves show the present α/N values calculated for pure TMS and Xe.

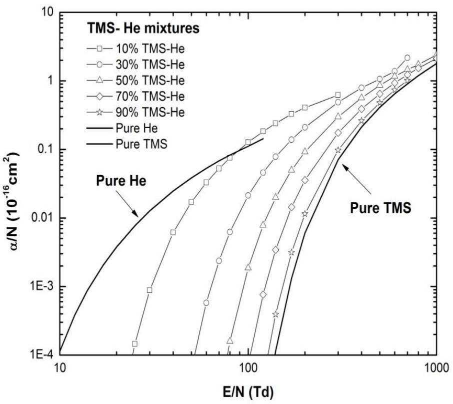

Fig. 15. The first Townsend ionization coefficient, α/N, as a function of E/N for the TMS-He mixtures with 10%, 30%, 50%, 70%, and 90% TMS. The solid line and symbols show present α/N values calculated using a two-term approximation of the Boltzmann equation for the TMS-He mixtures. The solid curves show the present α/N values calculated for pure TMS and He.

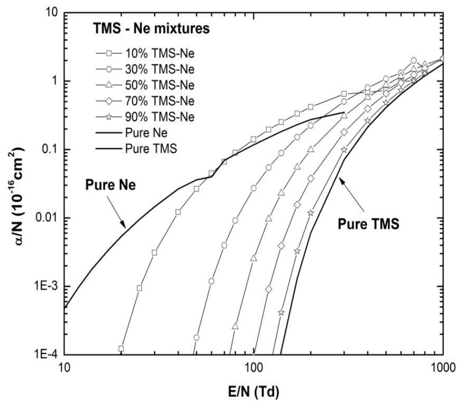

Fig. 16. The first Townsend ionization coefficient, α/N, as a function of E/N for the TMS-Ne mixtures with 10%, 30%, 50%, 70%, and 90% TMS. The solid line and symbols show present α/N values calculated using a two-term approximation of the Boltzmann equation for the TMS-Ne mixtures. The solid curves show the present α/N values calculated for pure TMS and Ne.

4 Conclusion

The electron transport coefficients (electron drift velocity, density-normalized longitudinal diffusion coefficient, ratio of longitudinal diffusion coefficient to electron mobility, Townsend first ionization coefficient) in mixtures of TMS gas with inert gases such as Kr, Xe, He and Ne gases in the E/N range of 0.1-1000 Td were calculated and analyzed for the first time using the two-term approximation of Boltzmann equation. These results were obtained based on accurate electron collision cross section sets for TMS molecule, Kr, Xe, He, and Ne atoms. Therefore, the present results are useful and necessary for many industrial applications, especially in plasma polymerization and plasma enhanced chemical vapour deposition.

Acknowledgments

This research was supported by Center for Research and Applications in Science and Technology, Hung Yen University of Technology and Education, under grant number UTEHY.T014.P1718.25.

References

1. Bordage M C *Plasma Sci. Tech* **9** 756 (2007)
2. Yoshida K, Mori S, Kishimoto Y, Ohuchi H, Hasegawa H, Shimozuma M and Tagashira H *J. Phys. D: Appl. Phys* **38** 1918 (2005)
3. Yanguas-Gil Á, Barranco Á, Cotrino J, Gröning P and González-Elipe A. R *Chemical Vapor Deposition* **12** 728 (2006)
4. Hunter S R, Carter J G and Christophorou L G *J. Appl. Phys.* **65** 1858 (1989)
5. Vinodkumar M, Korot K, Limbachiya C and Antony B. K *J. Phys. B* **41** 245202 (2008)
6. Krečmarová M J, Petrák V, Taylor A, Sankaran K J, Lin I N, Jäger A, ... and Vacík J *physica status solidi* **211** 2296 (2014)
7. Knoops H C, Braeken E M, de Peuter K, Potts S E, Haukka S, Pore V and Kessels W M *Appl. Mater. Interfaces* **8** 19857 (2015)
8. Kawaguchi S, Takahashi K, Satoh K and Itoh H *Plasma Sources Science and Technology* **26** 054001 (2017)
9. Mori H and Tachikawa H *Surf. Coat. Technol.* **149** 224 (2014)
10. Ando J, Ohmori T, Murase A, Takahashi N, Yamaguchi T and Hokkirigawa K, *Wear.* **266** 247 (2009)
11. Grotjahn T, Aslanbas Ö, Mee M, König M and Meier S *Surf. Coat. Technol.* **237** 134 (2013)
12. Soum-Glaude A, Thomas L, Dollet A, Ségur P and Bordage M C, *Diam. Relat. Mat.* **16** 1263 (2006)
13. Steven F D and Mário A B M *Journal of Vacuum Science & Technology A: Vacuum, Surfaces, and Films*. **16** 513 (1998)
14. Hien P X, Tuan D A and Jeon B H *J Korean Phys Soc*. **61** 72 (2012)
15. Hayashi M *J. Phys. D*. **15** 1418 (1982)
16. Hashimoto T and Nakamura Y, **ED-90-61** (Japan: IEE) as quoted in Suzuki M, Taniguchi T, Yoshimura N, and Tagashira H *J. Phys. D.* **25** 56 (1992)
17. Tagashira H, Sakai Y and Sakamoto S *J. Phys. D: Appl. Phys*. **10** 1063 (1977)
18. Tuan D A *J Korean Phys Soc* **64** 23 (2013)
19. Hien P X, Jeon B H and Tuan D A *J. Phys. Soc. Jpn* **82** 034301-1-8 (2013)